Lasers in Manufacturing Conference 2015

Shorter than short: How does the pulse duration influence the process efficiency of conductive materials?

S. Russ[a]*, R. Gebs[a], L. Bauer[a], U. Keller[a], T. Meyer[a], J. Roller[a], B. Führa[a], B. Faisst[b]

[a]*TRUMPF Laser GmbH , Aichhalder Straße 39, 78713 Schramberg, Germany*
[b]*TRUMPF Laser- und Systemtechnik GmbH, Johann-Maus-Str. 2, 71254 Ditzingen, Germany*

Abstract

Material micro processing with ultrashort laser pulses has been established during the last few years. There are a lot of processes that ultrashort pulsed (USP) lasers can be used for. Drilling of injection nozzles and cutting of Nitinol stents are already established in production lines. Other examples for the use of those kinds of lasers are scribing of silicon as well as processing of hard and brittle transparent materials. The range of possible applications is huge and nevertheless the micromachining market is still in its infancy. For many years since the invention of USP based material micro processing, pulse durations in the range of ten picoseconds were considered as the optimum choice for micro machining applications regarding process quality (Dausinger, Hügel, & Konov, 2003).
In scientific laboratories a well known technique to decrease the pulse duration of high power lasers from the picosecond into the femtosecond regime was based on chirped pulse amplification (CPA) since many years (Strickland & Mourou, 1985). However, this technique for a long time was too expensive to transfer it to industrial reliable high power lasers.
Today there are cost efficient and reliable high power CPA based femtosecond laser sources available for the industry. This ability seems to offer new micromachining opportunities for better quality and often also for even higher efficiency.
We have examined the influence on the efficiency and the quality for an ablation process on conductive materials. Therefore the pulse duration was reduced from 6 ps to 900 fs and even down to 400 fs.
By comparing those three pulse durations it will be much easier to decide which laser should be used for a certain process and material. And on the other hand it offers a good chance to discover new applications for lasers with ultrashort pulses.

Keywords: micro processing; picoceconds; femtoseconds; ultrashort pulses; ablation process

* Corresponding author. Tel.: +49 7422 515-8279; fax: +49 7422 515-401.
E-mail address: simone.russ@de.trumpf.com.

1. Introduction

In the last few years a lot of manufacturing processes in industry could be transferred to laser machining steps having the benefits of better process accuracy and often higher processing speed than conventional processes. Besides already well known processes like drilling of injector holes (Mielke, 2013) ablation processes came up over the last few years which also can be machined by ultrashort pulsed lasers e.g. assembling of air bearings. It is well known, that there are lasers sources available with different pulse durations for micromachining processes. The pulse duration of that kind of lasers has a huge influence on the process both on the quality and on the energy specific volume (efficiency). To increase speed it can be an advantage to work with pulse durations below 10 ps. But it is predicted that also with pulse durations in the range between 400 fs and 1000 fs depending on the material sometimes the ablation rate and the energy specific volume can be improved (Ancona, et al., 2009), (Lopez, et al., 2012), and (Neuenschwander, Jaeggi, Schmid, Rouffiange, & Martin, 2012). For industrial micro processing applications it is thus necessary to know which the best pulse duration for a defined process is. Besides the pulse duration a lot of other criteria influence the ablation process e.g. material properties and fluences. In this work we investigated the ablation behavior of three different pulse durations on stainless steel. We report on laser ablation with pulse durations of 400 fs, 900 fs and 6 ps at 1030nm.

2. Ablation Mechanism in Consideration of Pulse Duration

If the pulse duration exceeds more than 10 ps a thermal process can take place depending on material constants. This was already described by (Chichkov, Momma, Nolte, Alvensleben, & Tünnermann, 1996). Caused by thermal diffusion a heat affected zone begins to appear besides the laser-matter-interaction area. At this pulse durations the material first begins to melt before it is being vaporized.

For pulse durations below 10 ps typically the two temperature model is used to describe the ablation process. In this context the temperature of the electrons is considered independently from the lattice. The temperature of the excited electrons rises very fast because of their low mass. The temperature of the lattice is less than the electron temperature. At the end of a laser pulse the lattice temperature is approximately equal to the electron temperature (Chichkov et. al, 1996). The electron-phonon-coupling time τ_{ep} for iron for instance is 0.5 ps whereby for copper it takes 50 ps (Breitling, Ruf, & Dausinger, 2004). Pulses in the regime of picoseconds are accompanied by electron heat conduction whereat a short liquid phase and also a direct vaporization take place (Chichkov et. al, 1996). How efficient and precise lasers in this pulse duration regime are depends on the material and on certain other process parameters.

If the pulse duration is in the range of 400 fs to 900 fs it is for most materials shorter than the electron cooling time. Then the electron-phonon coupling time τ_{ep} can disregarded. That means the pulse is already decayed before the electrons transfer their energy to the lattice. Therefore nearly no melting phase is generated and a sublimation process can take place (Chichkov et. al, 1996).

But even if the pulses are shorter than one picosecond it is possible to generate melt and heat affected zone during a laser process when the process parameters aren't used in an optimum regime. As already (S. Nolte et. al, 1997) described there are two different ablation regimes concerning the fluence. If the fluence is below a certain material specific value, only the optical penetration depth is responsible for the ablation volume. In this fluence regime no melt and no heat affect appears. An increase of the fluence leads to higher energy penetration depths, which at this point cannot be described as optical penetration depth but as thermal penetration depth. Samples which are done in this regime show an influence of heat like melt or a decrease of ripples (S. Nolte et. al, 1997). Because the process with USP lasers is not only dependent on the pulse duration but also on other process parameters especially the laser fluence. This experimental work was done to especially compare three ultra short pulsed lasers at 6 ps, 900 fs and 400 fs with regard to their ablation behavior.

2.1. Ablation Law with a Gaussian Beam

As described above the laser process with ultra short pulses is not only influenced by the pulse duration but also by the laser fluence. There is a direct link between the fluence Φ and the energy penetration depths δ (described by (S. Nolte et. al, 1997) (Neuenschwander et. al, 2012))

$$Z_{abl} = \delta \cdot \ln(\Phi / \Phi_{th}) \quad (1)$$

In this context the ablation depths Z_{abl} is describable with the correlation from the energy penetration depth δ, the used laser fluence Φ and the threshold fluence Φ_{th}. The energy penetration depth shows how far the laser energy can penetrate into the material (Jaeggi, et al., 2011). If the threshold fluence is undercut it is not possible to ablate material. To determine the threshold fluence Φ_{th} the intensity profile of a Gaussian laser beam, has to be considered. In most cases the beam profile of piko and femtosecond lasers are given by this distribution:

$$I(r) = I_0 \cdot e^{\frac{-2r^2}{\omega_0^2}} \quad (2)$$

The intensity profile $I(r)$ is dependent on the distance r to the center of the laser beam, the parameter ω_0 defines the spot radius and I_0 is the maximum of the intensity. The intensity can be replaced by the peak fluence Φ_0, which is two times the pulse energy E_p divided by the spot area ($\pi \cdot \omega_0^2$). Hence this leads to the following expression.

$$\Phi(r) = \frac{2 \cdot E_p}{\pi \cdot \omega_0^2} \cdot e^{\frac{-2r^2}{\omega_0^2}} \quad (3)$$

Replacing Φ(r) by Φ_{th} leads in consequence to this expression.

$$\Phi_{th} = \Phi_0 \cdot e^{\frac{-2r^2}{\omega_0^2}} \quad (4)$$

By solving this equation for r it leads to the maximum for the spot radius at this laser fluence. By doubling and squaring this radius that in turn leads to the following correlation which was already described by (Mannion, Maggee, Coyne, & O'Connor, 2003).

$$D^2 = 2\omega_0^2 \ln(\Phi_0 / \Phi_{th}) \quad (5)$$

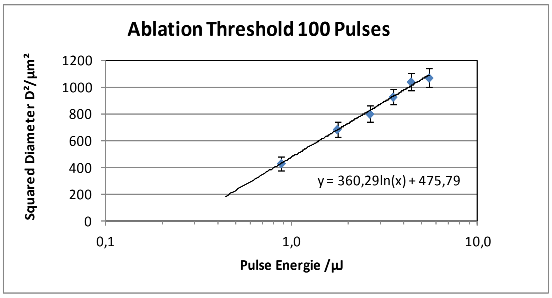

Fig. 1. Ablation threshold applied for 100 pulses

With this equation the connection between the squared diameter and the threshold is described. To find the threshold fluence it is better to plot the squared diameter D^2 versus the pulse energy Ep. The cross section with the x-axis and the plot can be used to figure out the threshold fluence, because of the link between energy and fluence Φ by the spot area ($2*Ep/\pi*\omega_0^2$) (Mannion et. al, 2003). In Fig. 1 an example for a plot which can be used for a determination of a threshold is shown. The ablation threshold decreases with the number of incoming pulses which is caused by changes of the surface characteristic. This can be described by an incubation effect and was already mentioned by (Jee, Michael, Becker, & Walser, 1988)

$$\Phi_{th}(N) = \Phi_{th,1} \cdot N^{S-1} \tag{6}$$

In this equation $\Phi_{th,1}$ is the indicator for the threshold fluence for a single pulse. N denotes the number of applied pulses and S is the incubation coefficient (Jaeggi, et al., 2011), (Neuenschwander et. al, 2012). For a good estimation of S the measurement should be done with at least 5 points.

As already described it is necessary to control the process by the used fluence, because it can influence the process and the maximum ablated volume at certain used pulse energies. For pulse durations shorter than 6 ps it is predicted by (Neuenschwander et. al, 2012) that the threshold fluence stays more or less constant for a certain number of applied pulses. If the ablation rate increases for shorter pulse durations this cannot be explained only by the ablation threshold but on the penetration depth which is dependent on the pulse duration also. The question is, if a reduction from 900 fs to 400 fs leads to a rise of the ablation rate and how much the ablation rate can be increased.

3. Experimental Set Up

In this work three different lasers were used for the investigation. Therefore a picosecond laser with 6 ps, a femtosecond laser with 900 fs and one with 400 fs have been compared for the tests. The pulse durations were measured by an autocorrelator.

All tests were done with lasers from the TRUMPF TruMicro 5000 Series. In this series there are picosecond and femtosecond lasers with pulse durations <10 ps and 900 fs specified. The laser with 400 fs was just built up for laboratory tests and isn't available as a product up to now.

3.1. The Specifications of the used Lasers

The picosecond laser was a TruMicro 5070 with 100 W average power which offers a pulse duration of ~6 ps at a wavelength of 1030 nm. This laser is based on a regenerative Yb:YAG thin disc amplifier. Core of this laser is a thin disk laser module which normally is used for cw- disk lasers. The pulses are generated in a mode locked fiber seed oscillator and after picking them they are being amplified via the regenerative amplifier. The amplified pulses are coupled out with the help of an intracavity electro optic modulator (EOM). This EOM allows realizing different repetition rates and thus different pulse energies. An additional external EOM allows amplitude modulation of the pulse energy and the number of extracted pulses working as a pulse divider. Furthermore this external EOM enables to linearize and stabilize the output power of the laser (Heckl, et al., 2014). The base frequency of the used lasers can be set to 400, 600 and 800 kHz which in turn delivers different pulse energies at the same average power.

The 900 fs laser which was used for those tests was a TruMicro 5050 Femto Edition with 40 W average power based on CPA (Strickland & Mourou, 1985). In this laser a femtosecond seed pulse was first stretched and afterwards amplified in the same kind of thin disk based regenerative amplifier mentioned above. This TruMicro 5050 Femto Edition provides the same external EOM as the picosecond laser mentioned above. After the regenerative amplifier a compact single pass compressor reduces the pulse duration back to 900 fs as described in (Heckl, et al., 2014). This laser also can deliver four different base frequencies (200, 400, 600 and 800 kHz) at a wavelength of 1030 nm.

The laser with a pulse duration of 400 fs was built up at the same platform as the TruMicro 5050 Femto Edition. It also delivers 40 W average power and works in a similar way as the 900 fs laser. To reach the shorter pulse duration nonlinear spectral broadening was additionally introduced into the regenerative amplifier scheme. This laser was designed for two different internal frequencies (600 and 800 kHz) and also emitted pulses at 1030 nm.

3.2. Ablation Trials

For the ablation trials the three lasers were used, described above. To focus the laser beam and generate high feed rates on the work piece a scanner head with a 100 mm telecentric focal lens was used. The lasers are combined with high accuracy micromachining stages for positioning in x, y and z- direction. The laser beam is guided by mirrors to use it at the focusing unit. With a beam switch it is possible to change between the lasers without modifying the optical setup (Fig. 2)

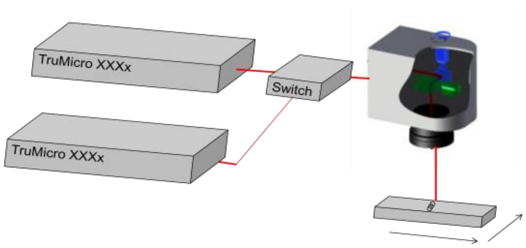

Fig. 2. Lasers can be chosen by a beam switch. A scanner head (Picture Fraunhofer ILT) was used to move the laser beam

For the ablation trials small grooves with different speeds were done on 1 mm stainless steel sheets. To get a certain depth each groove was repeated 10 times. The tests were done at different speeds and three different frequencies to change the temporal and the spatial spot distance. To compare the results all grooves were analyzed after the laser process by a laser scanning microscope.

4. Experimental Results

4.1. Ablation Experiments and Calculations for Stainless Steel

In a first step the ablation threshold for stainless steel was determined as described above by the method of Mannion et. al, 2003. For this material the thresholds were plotted for 1, 5, 10, 25, 50 and 100 pulses per spot respectively to describe the incubation effect explicated above with equation (6). The ablation thresholds for 200 pulses were figured out afterward from the plot. The left chart in Fig. 3 shows one of the results of those investigations exemplified for 900 fs. The right chart in Fig. 3. shows the comparison of the ablation thresholds for 200 applied pulses for all three lasers. The theory that the ablation threshold doesn't change much for a rising number of pulses below a duration of 10 ps could be confirmed by the plots. For 200 applied pulses the threshold reaches nearly the same level for all lasers (Neuenschwander et. al, 2012).

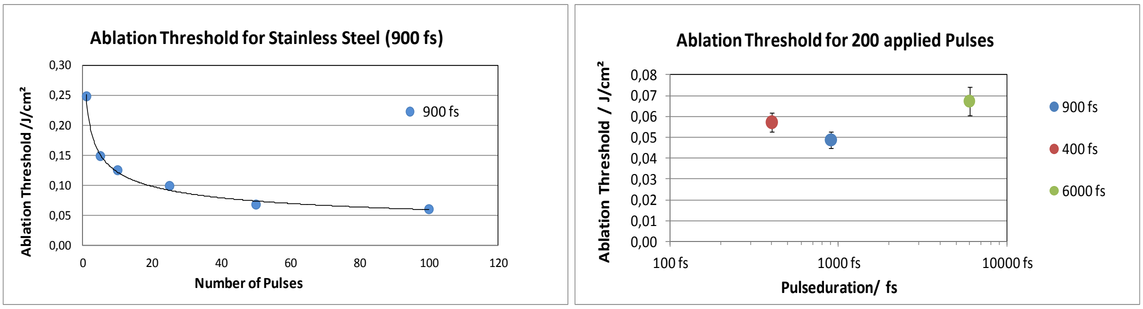

Fig. 3. Left chart: Ablation threshold Φ_{th} depicted as functions of the number of applied pulses for stainless steel for 900 fs. Right chart: Comparison of the ablation threshold for 200 applied pulses (400 fs, 900 fs and 6 ps).

In a second step the ablation experiments on stainless steel were carried out. To compare the ablation results these tests were done at the same fluence, pulse overlap and same frequency, respectively. The fluence (average fluence) was varied first from 0.15 J/cm² to 4 J/cm² (peak fluence 0.3 J/cm² to 8 J/cm²) whereby the pulse overlap was set at 80 %. The frequency was adjusted to 800 kHz. To compare the results the ablated volume per pulse was calculated and plotted versus the fluence. To calculate the volume per pulse, the volume of a certain length of the groove was determined by measuring the cross section of the groove by a laser scanning microscope and multiplying by the length. In a second step this volume was divided by the number of applied pulses, which gives an average volume for each pulse. To get an impression of the ratio between the incoming energy and the ablated volume per pulse a second plot was created. With those two comparisons of the values it was possible to get an impression of the process results. The charts are shown in Fig. 4.

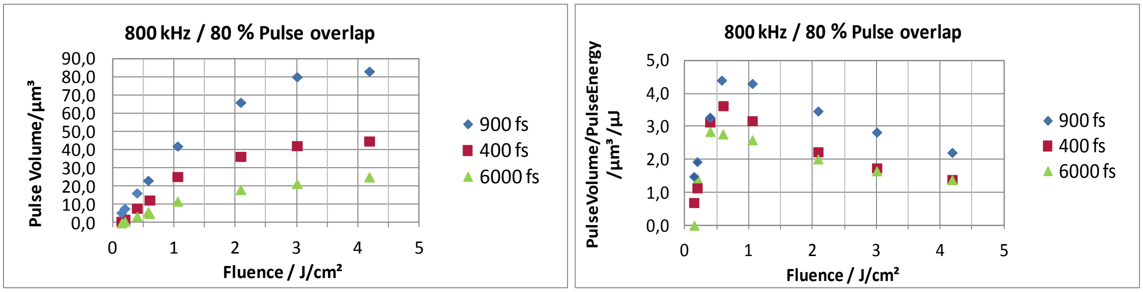

Fig. 4. Left Chart: ablated volume per pulse, right chart: ratio of ablated volume per pulse and pulse energy

The left chart shows the ablated volume per pulse plotted versus the used average fluence. In the right chart the ratio of the ablated volume per pulse and the used pulse energy (in the following named as energy specific volume) also was printed versus the fluence, which was varied in the same range as described above. In both charts the results of the three investigated lasers are summarized whereby the blue rhomb is used for the 900 fs laser, the red rectangle for the 400 fs laser and the green triangle for the 6 ps laser.

These first results show that the ablated volume for the 900 fs laser is higher than for the 400 fs and for the 6 ps laser. Looking at the energy specific volume it also can depicted that the highest value could be reached with 900 fs at around 0.6 J/cm² (average fluence). In a first impression those values seem to be confusing thinking about the theory that the energy penetration depth for femtosecond pulses should increase for shorter pulses ((Neuenschwander et. al, 2012),(Chichkov et. al, 1996)). Those values let assume that the penetration depth for 900 fs should be higher than for 400 fs. But similar results also had been mentioned by (Lopez, et al., 2012) where they found a higher process efficiency for pulse durations in the range of 1 ps for stainless steel.

To get a better process understanding a lot of similar tests were done by varying the pulse overlap, the frequency and the fluence from 0.58 to 4.19 J/cm². They all showed the same result, that the ablated volume with 900 fs exceeds the 400 fs value in all executed measurements.

Assuming that the energy penetration depth could be affected on the scanning speed and the repetition rate it was recalculated by the number of the applied pulses per spot. For example at a pulse overlap of 75 % and 10 repetitions 40 pulses per spot are applied. Using the threshold Φ_{th} for 40 pulses from the incubation charts and measuring the depth Z_{abl} of the ablated grooves, all values are delivered to calculate the energy penetration depth δ from equation (1). The calulations showed that the energy penetration depth is rather similar for 400 fs and 900 fs. For example at 93 % pulse overlap and 800 kHz (around 140 pulses per spot) an energy penetration depth of around 9 nm was calculated for small fluences for 400 fs and 900 fs whereas it was quite lower for 6 ps. Further on the ablated volume per pulse was determined by using the following equation (Neuenschwander et. al, 2012)

$$\Delta V = \frac{1}{4} \cdot \pi \cdot \omega_0^2 \cdot \delta \cdot ln^2(\frac{\phi_0}{\phi_{th}}) \quad (7)$$

Inserting the values for the threshold fluence Φ_{th} for the same number of pulses than calculated from the pulse overlap and the corresponding energy penetration depth δ, the volume for each utilized peak fluence Φ_0 could be calculated by using ω_0 for the spot radius.

The results show that the data found in the ablation experiments for 400 fs, 900 fs and 6 ps could be confirmed approximately by the calculation.

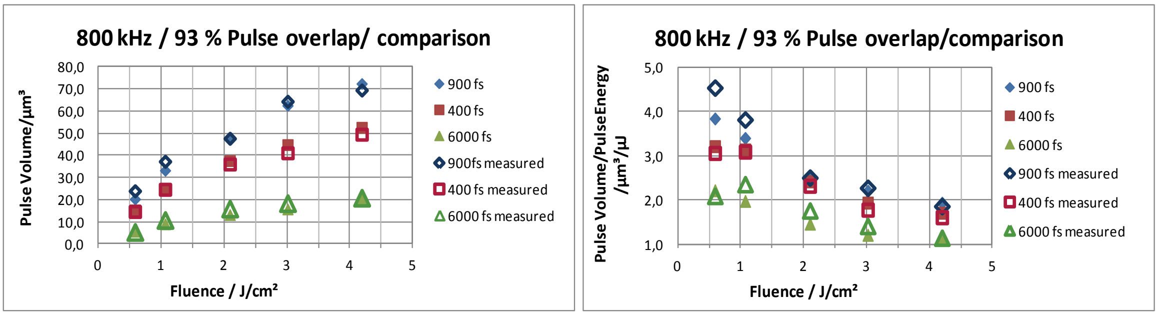

Fig. 5: The charts show as well the measured and the calculated values for the pulse volume V_p and the energy specific volume V_p/E_p. The measured values are illustrated by blank geometrical shapes. The calculated ones are filled. The carts were done for 800 kHz and a pulse overlap of 93 %.

Fig. 5 shows a first example for the comparison between the measured data and the calculated data. On the left side the values for ablated volume per pulse are illustrated whereas on the right side the energy specific volume results are shown. The charts show as well the measured and the calculated data for all three lasers at a frequency of 800 kHz and a pulse overlap of 93 %. There are red rectangles for the 400 fs laser, blue rhombs for the 900 fs laser and green triangles for the 6 ps laser. For each laser the measured data points are indicated by blank marks and the calculated values are represented by the filled ones. The charts show that the measured and calculated data for all three lasers fit quite well.

Those results indicate that the ablated volume for 400 fs is below the values of 900 fs but above 6 ps, which could be confirmed also by calculation. The energy specific volume for 400 fs seems to converge for fluences greater than or equal to 2 J/cm² to the values of 900 fs. To emphasize these impressions further investigations were done at different conditions.

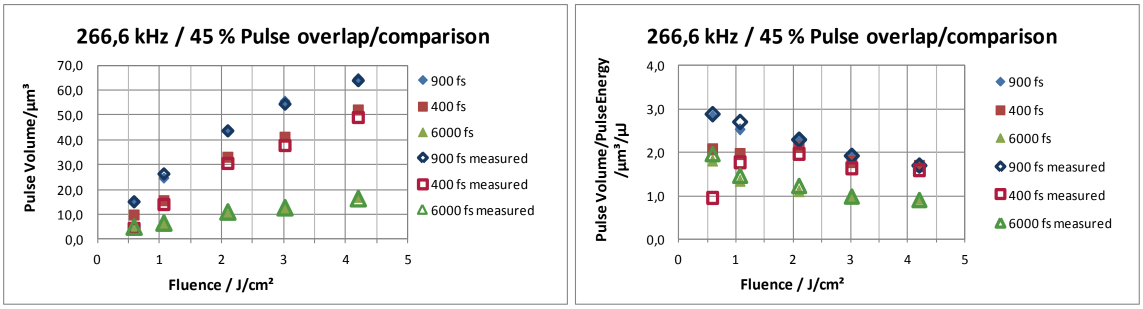

Fig. 6: Calculated/measured values (400 fs) for the pulse volume and the energy specific volume for 266 kHz and P_o of 45 % (cf. Fig. 7)

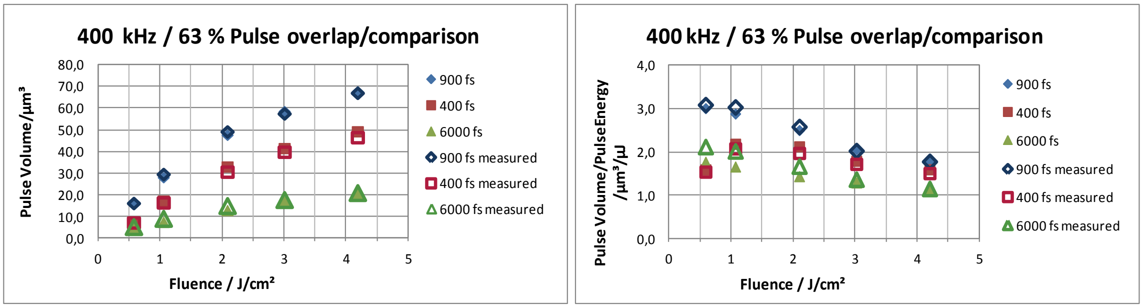

Fig. 7. The charts show as well the measured and the calculated values for the pulse volume V_p and the energy specific volume V_p/E_p. The measured values are illustrated by blank geometrical shapes. The calculated ones are filled. The carts were done for 400 kHz and a pulse overlap of 63 %.

Fig. 6 and Fig. 7 show additional charts done for other pulse overlaps and frequencies f (f = 266 kHz and pulse overlap 45% as well as for f = 400 kHz and pulse overlap 63%).

Also these results show that the values for 400 fs, 900 fs and 6 ps could be confirmed by the calculation. The deviations could be explained by errors which occur by means of measurement as well for the depth and volume of the groove. Obviously the results show, that there is an influence concerning the pulse overlap and the frequency on the ablated volume and the energy specific volume. Considering the calculated volume for 900 fs it seems to decrease for lower pulse overlaps. Whereas the value for 400 fs stays almost stable for all investigated pulse overlaps and frequencies for fluences greater or equal to 2 J/cm². At lower fluences the ablated volume per pulse also decreases for 400 fs at lower pulse overlaps (reduction by half compared at 266 kHz/45 % to 800 kHz/93 %). Therefore in the lower fluence regime the energy specific volume at 400 fs deviates stronger from 900 fs and also from 6 ps for lower pulse overlaps and frequencies. But for fluences above 2 J/cm² the energy specific volume for 400 fs and 900 fs begins to converge again also for the measured and for the calculated values (Fig. 5 - Fig. 7).

For all compared data points the values for the 400 fs laser are on a lower level than the data for 900 fs but in most cases higher than the 6 ps results. The investigation is also confirmed by calculation where the ablated volume for 400 fs in neither case could exceed the 900 fs level. This method of calculation confirms the ablation results for all three lasers.

It has to be pointed out, that the energy penetration depth at 400 fs and 900 fs during a laser process seems to be quite similar. On the other hand the ablated volume (7) does not consider just the energy penetration depth δ but also the threshold fluence Φ_{th} for the number of applied pulses. For the investigated lasers the ablation thresholds are a little bit different. This lead to the effect, that even for a similar penetration depth at 400 fs the ablated volume per pulse nevertheless is lower than at 900 fs (cf. Fig. 5 - Fig. 7).

The measured and the calculated volume and energy specific volume for 400 fs are in all cases below the values for 900 fs, therefore it can be assumed that there are effects which influence the penetration depth at 400 fs during the process. For example nonlinear effects could influence the ablation results as published by (Breitling, K.-P.Müller, A.Ruf, P.Bergner, & Dausinger, 2003) and (Breitling, Ruf, & Dausinger, 2004). They identified a higher disturbance during a process by using pulses below one picosecond. They detected a distorting influence on the beam profile for pulses from 500 fs and shorter. This distorting effect of the beam profile led to an irregular ablation. At this point there are only assumptions that such effects probably have a negative effect on the ablated volume of stainless steel.

In addition the fast temporal increase of the intensity at 400 fs may lead to a shielding effect during the ablation process especially for this material. This could mean that material specific parameters and the temporal pulse formation may interfere with each other in a negative way.

5. Conclusion

In this work the ablation thresholds following (Mannion et. al, 2003) on stainless steel have been investigated for three different pulse durations at 400 fs, 900 fs and 6 ps. The incubation effect was determined by the method of (Jee et. al, 1988) and in a good agreement to (Neuenschwander et. al, 2012) the threshold fluences for a high number of applied pulses reached nearly the same value for the investigated lasers. Further on ablation experiments with the same material were carried out to determine the ablated volume per pulse and the energy specific volume. For the ablation experiments grooves were engraved by using a galvo scanner and focusing by an f-theta objective. Different pulse overlaps and frequencies were used to vary the spatial and temporal pulse to pulse distance on the work piece. The ablated volume per pulse and the energy specific volume were plotted versus the average fluence. The results showed a disproportion to the assumption that the energy penetration depth should be higher for 400 fs and that the energy penetration depth is the leading factor for pulses below one picosecond.

Calculations of the energy penetration depth and the ablated volume showed a good agreement for 400 fs, 900 fs and 6 ps with the real ablated volume. But with 400 fs the ablated volume could exceed in neither case the ablated volume of 900 fs. This led in the end to the assumption that the ablation process at 400 fs could be influenced by some not confirmed effects like nonlinear((Breitling et. al, 2003), (Breitling, Ruf, & Dausinger, 2004)) or shielding effects which may caused by an interplay between the material and the temporal pulse formation.

To get more process understanding it would be necessary to do more detailed investigations. It is planned to do high speed videos of the process and ablation experiments of areas instead of grooves. Also other materials should be investigated to compare the results and look for similar effects. Nevertheless it is not completely understood why the ablated volume at 400 fs is below 900 fs. The investigation helped to get a better appreciation of the process behavior of ultra short pulses when ablating stainless steel.

References

Ancona, A., Döring, S., Jauregui, C., Röser, F., Limpert, J., Nolte, S., & Tünnermann, A. (November 2009). Femtosecond and picoseconds laser drilling of metals at high repetition rates and average powers. *Optics Letters, Vol. 34, No. 21*.

B.Neuenschwander, G.Bucher, B.Joss, Muralt, M., & et.al, M. U. (2010). Processing of dielectric materials and metals with ps-laserpulses: results, strategies limitations and needs. *Proceedings of SPIE vol 7584*.

Breitling, D., K.-P.Müller, A.Ruf, P.Bergner, & Dausinger, F. (2003). Material-vapor dynamics during ablation with ultrashort pulses. *Proc. SPIE 5063*, S. 81-86.

Breitling, D., Ruf, A., & Dausinger, F. (2004). Fundamental aspects in machining of metals with short and ultrashort laser pulses. *Proc. Of SPIE Vol. 5339 (SPIE, Bellingham, WA)*.

Chichkov, B., Momma, C., Nolte, S., Alvensleben, F. v., & Tünnermann, A. (1996). Femtosecond, picosecond and nanosecond laser ablation of solids. *Appl. Phys. A 63*, S. 109.

Dausinger, F., Hügel, H., & Konov, V. (2003). Micro-machining with ultrashort laser pulses: From basic understanding to technical applications. *Proc. SPIE Vol. 5147*, S. 106-115.

Heckl, O., Weiler, S., Fleischhaker, R., Gebs, R., Budnicki, A., Wolf, M., . . . Sutter, D. (March 2014). Industry-grade High Average Power Femtosecond Light Source. *Proc. Of SPIE Vol. 8972*.

Jaeggi, B., Neuenschwander, B., Schmid, M., Muralt, M., Zuercher, J., & Hunziker, U. (2011). Influence of the Pulse Duration in the ps-Regime on the Ablation Efficiency of Metals. *Physics Procedia 12*, S. 164–171.

Jee, Y., Michael, F., Becker, F., & Walser, R. M. (March 1988). Laser-induced damage on single-crystal metal surfaces;. *J. Opt. Soc. Am. B/Vol. 5, No. 3*.

Lopez, J., Kling, R., Torres, R., Lidoff, A., Delaigue, M., Ricaoud, S., . . . Mottay, E. (2012). Comparison of picosecond and femtosecond laser ablation for surface engraving of metals and semiconductors. *Proc. Of SPIE Vol. 8243 82430O-1*.

Mannion, P., Maggee, J., Coyne, E., & O'Connor, G. M. (2003). Ablation thresholds in ultrafast laser micro-machining of common metals in air. *Proceedings of SPIE Vol. 4876*, S. 470-478.

Mielke, M. (2013). The hole story: Femtosecond manufacturing improves automobile fuel efficiency. *Laser Focus World*.

Momma, C., Nolte, S., Chichkov, B., Alvensleben, F., & Tünnermann, A. (1997). Precise laser ablation with ultrashort pulses. *Appl. Phys. Sci.109/110*, S. 15-19.

Neuenschwander, B., Jaeggi, B., Schmid, M., Rouffiange, V., & Martin, P. (2012). Optimization of the volume ablation rate for metals at different laser pulse-durations form ps to fs. *Proc. Of SPIE Vol. 8243*.

S. Nolte et. al, C. M. (October 1997). Ablation of metals by ultrashort laser pulses. *J. Opt. Soc. Am. B/ Vol. 14*, S. 2719.

Sanner, N., Uteza, O., Bussiere, B., Coustillier, G., Leray, A., Itina, T., & Sentis, M. (2008). Measurement of femtosecond laser-induced damage and ablation thresholds in dieslectrics. *Appl Phys A*.

Strickland, D., & Mourou, G. (1985). Compression of amplified chirped optical pulses. *Opt. Commun. 56*, 219.